Polymers for Advanced Technologies

WILEY

polymers advanced technologies

RESEARCH ARTICLE OPEN ACCESS

Mechanical Behavior Prediction of 3D-Printed PLA/Wood Composites Using Artificial Neural Network and Fuzzy Logic

Osman Ulkir[1] | Gazi Akgun[2] | Arif Karadag[3]

[1]Department of Electric and Energy, Mus Alparslan University, Mus, Turkey | [2]Department of Mechatronics Engineering, Marmara University, Istanbul, Turkey | [3]Department of Motor Vehicles and Transportation Technologies, Mus Alparslan University, Mus, Turkey

Correspondence: Osman Ulkir (o.ulkir@alparslan.edu.tr)

Received: 16 December 2024 | **Revised:** 25 January 2025 | **Accepted:** 30 January 2025

Funding: The authors received no specific funding for this work.

Keywords: additive manufacturing | artificial neural network | FDM | fuzzy logic | PLA/wood

ABSTRACT

This study presents a novel approach to optimize and predict the mechanical properties of 3D-printed polylactic acid (PLA)/wood composites through artificial neural network (ANN) and fuzzy logic (FL) modeling. The research addresses the critical challenge of determining optimal process parameters in fused deposition modeling (FDM) of natural fiber composites. Using Taguchi's L27 orthogonal array, experiments were conducted with five key printing parameters: layer thickness (100–200–300 μm), printing speed (PS) (40–60–90 mm/s), raster angle (RA) (0°–45°–90°), infill density (ID) (30%–60%–90%), and nozzle temperature (NT) (190°C–200°C–210°C). Analysis revealed that RA and PS were the most influential parameters, contributing 41.86% and 40.92% to tensile and compressive strengths, respectively. The developed ANN model demonstrated exceptional prediction accuracy with R^2 values of 99.94% for both tensile and compressive strengths, surpassing the FL model's performance ($R^2 = 97.16\%$). The development of these models is crucial for accurately predicting mechanical behavior, allowing for efficient process optimization without extensive physical testing. Both methods demonstrated high prediction accuracy. Validation tests revealed that maximum errors of 1.95% and 2.81% for ANN and FL, respectively. The findings contribute valuable insights for the development of high-performance natural fiber composites and establish a foundation for future advanced manufacturing processes.

1 | Introduction

Additive manufacturing (AM), commonly known as 3D printing, has transformed traditional manufacturing by enabling the production of complex geometries, customized designs, and lightweight structures with minimal material waste [1, 2]. Its versatility and efficiency have led to widespread adoption across industries such as aerospace, automotive, healthcare, and consumer goods [3–5]. Fused deposition modeling (FDM) is notable among AM technologies for its affordability and versatility in processing various thermoplastics, such as polylactic acid (PLA), acrylonitrile butadiene styrene (ABS), and reinforced composites [6]. The integration of natural fibers, such as wood, into polymer matrices has gained attention for its environmental benefits, including biodegradability, a low carbon footprint, and cost-efficiency [7, 8]. Wood–polymer composites (WPCs), particularly those based on PLA, are increasingly used in sustainable manufacturing applications, such as furniture, interior design, decorative components, and lightweight structural elements [9, 10].

In FDM-based 3D printing, selecting appropriate process parameters is crucial for ensuring quality and performance [11, 12]. Factors such as infill density (ID), layer thickness (LT), nozzle temperature (NT), printing speed (PS), and raster angle (RA)

significantly affect the mechanical properties, surface texture, and dimensional accuracy of printed parts [13, 14]. Predicting and optimizing these parameters minimizes defects, such as voids, delamination, and poor interlayer bonding while maximizing the advantages of FDM, including material efficiency and cost-effectiveness. The mechanical behavior of PLA/wood composites under varying conditions is a key area of focus for their effective utilization. These materials offer a unique combination of PLA's durability and wood's aesthetic and sustainable qualities [15, 16]. However, challenges like anisotropic behavior and interfacial bonding complexities necessitate detailed investigations into properties such as tensile and compressive strength to predict and optimize their performance for applications in furniture, lightweight structures, and decorative elements [17, 18].

The predicting mechanical properties in FDM-manufactured parts is a critical area of research [13, 19]. The interdependence of printing parameters can lead to significant variations in the mechanical performance of printed components [20, 21]. Accurate predictions of properties like tensile and compressive strength allow manufacturers to optimize designs and production processes without extensive trial-and-error experimentation, saving time, and resources. Recent advancements in machine learning and artificial intelligence (AI) have further enhanced this field [22–25]. Techniques such as artificial neural networks (ANNs), genetic algorithms, and fuzzy logic (FL) are widely applied to understand the relationships between printing settings and resulting mechanical characteristics [26–28]. These tools can process complex datasets to identify patterns and make reliable predictions with high accuracy. The integration of AI-based predictive models helps manufacturers enhance parameter optimization and design customized approaches for materials like PLA/wood composites, supporting the industrial shift toward sustainable and high-performance material solutions.

There are not enough studies in the literature on improving and predicting tensile and compressive strength of PLA/wood composite materials using FDM process [29–33]. Fountas et al. investigated the effects of FDM parameters on the ultimate tensile strength (UTS) of PLA reinforced with wood flour [34]. Using Taguchi's design with orthogonal arrays, test specimens were fabricated per ASTM D638-10 standards, varying LT, NT, raster deposition angle, and PS. Stress–strain curves and UTS values were analyzed through statistical methods, including analysis of variance (ANOVA) and contour plots, to identify key parameter interactions. Full quadratic models demonstrated high accuracy in predicting UTS. Results were validated with micrographs of fracture surfaces and comparisons with studies on pure PLA, offering valuable insights into optimizing FDM parameters for biocompatible PLA/wood composites. Kelleci et al. investigated blends of polypropylene (PP) with biopolymers PLA and polyhydroxybutyrate (PHB), combined with wood flour, to identify the optimal composite properties using fuzzy and gray multicriteria decision-making (MCDM) methods [35]. They analyzed the physical, mechanical, thermal, structural, and morphological characteristics of composites. Results revealed that PLA and wood flour enhanced the mechanical properties of PP composites, although wood flour exhibited poor dispersion in the matrix. Thermal stability remained unchanged with PLA and PHB but improved with wood flour. Fuzzy and Gray MCDM analyses provided consistent rankings of the composite properties. Morvayová et al. developed a 3D-coupled thermomechanical numerical model to optimize FDM fabrication of PLA/wood biocomposites [36]. The model predicts dimensions, defect formation, residual stresses, and temperature profiles, addressing the need for tailored solutions for biocomposites. Validation with experimental data showed strong agreement, with a maximum relative error of 9.52% for dimensions and accurate defect prediction. This study advances the understanding of FDM processes for sustainable materials, offering a valuable tool for improving the quality of PLA-based biocomposites. Estakhrianhaghighi et al. developed wood fiber-reinforced PLA composites to enhance flexural properties and sustainability [37]. Incorporating 2.5%–15% wood fibers improved flexural modulus (60%), rigidity (72%), strength (39%), and failure strain (21%) while reducing density by 5.2%. Architected cellular beams, termed "Isoflex," achieved up to 130% higher specific flexural rigidity and 70% better isotropic flexural properties than pure PLA beams, showcasing WF-PLA as a sustainable solution for AM. Zandi et al. studied the flexural properties of Timberfill, a wood-reinforced PLA composite, using FDM and an L27 Taguchi design [38]. Layer height was the most influential parameter, followed by nozzle diameter and ID, with optimal settings achieving 47.26 MPa flexural strength. Wood fibers reduced PLA's cohesion, creating voids that decreased strength. Compared to injection molding, FDM improved resistance and elastic properties, with a 25% lower Young's modulus for FDM samples. Most existing studies on wood-based materials lack the development of predictive models for mechanical properties. The unique aspect of this study lies in the integration of the Taguchi experimental design with predictive modeling using ANN and FL. Through experiments designed using the Taguchi, the five most influential parameters were identified and used to develop accurate models for predicting tensile and compressive strength. This approach not only enhances the understanding of parameter effects but also provides a reliable framework for optimizing the mechanical performance of wood-based composites.

This study focuses on exploring the mechanical properties of FDM-printed PLA/wood composites and developing predictive models to optimize their performance. Using a Taguchi experimental design with five critical parameters—ID, LT, PS, NT, and RA—mechanical properties such as tensile and compressive strength were systematically investigated across 27 experimental runs. ANOVA was employed to identify the most influential parameters, revealing that RA significantly impacts tensile strength, while PS is critical for compressive strength. Its dual focus on experimental analysis and predictive modeling sets this research apart. This study employs ANN and FL to analyze the mechanical behavior of PLA/wood composites and create accurate and dependable prediction models. This integrated approach provides a comprehensive understanding of how FDM process parameters influence composite performance, paving the way for more efficient and sustainable manufacturing practices.

2 | Materials and Methods

2.1 | 3D Printing Process and Materials

The fabrication of the samples was performed using the FDM with wood-filled PLA composite material. The creality K1C 3D printer was utilized for this process. This printer can

process engineering materials such as PLA, ABS, and wood-filled composites. Key features of the printer include an extruder that can heat up to 300°C, compatibility with 1.75 mm filament diameter, and a heated bed that reaches temperatures up to 180°C. The printer supports a maximum print speed of 600 mm/s and achieves 0.1 mm precision, enabling efficient, high-quality production. The production workflow typically starts with the creation of a 3D model in computer-aided design (CAD) software. In this study, SolidWorks was used to design the models. The CAD model is then exported to standard tessellation language (STL) format, which represents the geometry of the design using triangular facets. This STL file is processed using slicing software to generate G-code, which contains instructions for the printer regarding movement paths, extrusion rates, and key settings such as temperature. The G-code guides the printer in sequentially depositing the material layer by layer, completing the production process. The fabrication process of all samples was performed with this method. Two types of samples were designed for testing: tensile and compression specimens. The tensile specimens were prepared according to ISO 527-Type 1A standards, while the compression specimens followed ASTM D695 standards. All samples were printed in the XY plane and loaded in the Z direction. The determination of printing parameters and levels was guided by the design of experiments (DoEs) approach. In addition, other parameters were kept constant during the production process. The constant parameters are detailed in Table 1.

In this study, Creality CR-Wood filament, a wood-filled PLA material, was used for FDM 3D printing. This filament combines PLA with fine wood particles, providing enhanced mechanical properties, a natural wood-like texture, and excellent printability with minimal warping. Operating at optimal temperatures between 190°C and 220°C, it offers lightweight yet robust parts and is environmentally friendly due to its biodegradable content. These features make it suitable for decorative models, structural prototypes, and eco-friendly products.

2.2 | Design of Experiments

The Taguchi methodology was used to minimize the number of tensile and compression test experiments while optimizing the manufacturing parameters. This approach is widely adopted in the development stages of processes to enhance efficiency, reduce costs, and improve product quality [39, 40]. The accurate selection of printing parameters is essential to enhance the mechanical properties and overall quality of the final product during production. For this purpose, the key process parameters influencing compression strength were investigated. Insights from previous literature, earlier experiments, and trial studies significantly contributed to identifying the fixed and variable parameters.

The fixed parameters identified for the study are listed in Table 1, while the variable parameters included ID, LT, PS, NT, and RA. These parameters were analyzed across different levels to understand their impact on the mechanical performance of the printed specimens. The factors and levels are detailed in Table 2. The maximum strength value obtained during the tensile and compression test served as the output parameter, representing the dependent variable in this analysis. The Taguchi L27 orthogonal array was employed to streamline the experimental process. This array is specifically designed to evaluate factors with three levels and includes a total of 27 experimental combinations. This design allows for an efficient analysis of the individual and combined effects of multiple factors by minimizing the number of required tests.

TABLE 1 | The fixed printing parameters during FDM.

Factors	Unit	Value
Nozzle diameter	mm	0.4
Table temperature	°C	60
Number of contours	integer	5
Raster width	mm	0.40
Infill pattern	—	Cubic

2.3 | Experimental Procedure

The mechanical properties of wood-filled PLA materials were evaluated through tensile and compression tests. The procedures for sample preparation and testing adhered to internationally recognized standards to ensure the accuracy and comparability of results. Tensile specimens were designed according to the ISO 527-Type 1A standard and fabricated using wood-filled PLA material through the FDM. The tensile strength, defined as the maximum stress a material can endure under tension before breaking, was measured. Testing was performed on an AG-X Shimadzu universal testing machine with a capacity of 50 kN. The test followed the specifications of the ISO standard with a pull speed of 1 mm/s. The machine's high accuracy (±0.1%) ensures precise stress–strain data recording. This setup provides insights into the elastic and plastic deformation behaviors of the material. Compression specimens were prepared following the ASTM D695 standard, using the same wood-filled PLA material and fabrication technique. The test aimed to determine the compressive strength of the material. The procedure was conducted using the AG-X Shimadzu test machine with a 50 kN capacity, at a constant loading rate of 1.3 mm/min as per standard guidelines. During the test, the specimens were carefully aligned between the machine's jaws to ensure uniform load distribution. The loading process involved the application of a gradually increasing compressive force, progressing through the elastic and plastic deformation regions until reaching the failure or permanent deformation point. The experimental results of the tensile and compressive strength are presented in Table 3. Since each sample was tested three times, the results in the table are the average of the tests performed.

2.4 | ANN Method

ANNs are computational models inspired by the biological neural networks found in the human brain [41]. These models are

TABLE 2 | The design parameters and their respective values.

Factors	Symbol	Units	Level 1	Level 2	Level 3
Infill density	ID	%	30	60	90
Layer thickness	LT	μm	100	200	300
Printing speed	PS	mm/s	40	60	90
Nozzle temperature	NT	°C	190	200	210
Raster angle	RA	°	0	45	90

designed to simulate the way the brain processes information, making them highly effective for solving complex problems involving nonlinear relationships. ANNs are widely used in data modeling and prediction tasks, where they learn from sample data to make accurate predictions, offering significant time and cost savings compared to traditional analysis methods. Unlike conventional methods that often require the entire dataset, ANNs rely on subsets of data for training, allowing for quick and efficient modeling. The structure of an ANN typically consists of three main layers: an input layer, one or more hidden layers, and an output layer [42–44]. The input layer receives the initial data, representing the independent variables or features of the system under study. Between the input and output layers, the hidden layer(s) perform complex computations by processing weighted inputs and generating outputs through activation functions. These activation functions introduce nonlinearity, enabling the network to model intricate patterns in the data. The output layer provides the final predictions or classifications based on the processed data from the hidden layer(s).

In this study, an ANN model was implemented to analyze and predict the behavior of 3D-printed materials. MATLAB was used to develop the ANN, which comprised an input layer with five inputs, three hidden layers operating under feed-forward backprop conditions, and a single output layer with two outputs. The network was trained using experimental data obtained from Table 4, ensuring the model's ability to accurately predict outcomes under various conditions. The ANN design and learning variables used in this study are given in Figure 1. The study employed ANNs to accurately model nonlinear dependencies between 3D-printing parameters and material properties, delivering key insights for process optimization. The approach demonstrates the versatility and robustness of ANNs in engineering applications, highlighting their potential as a powerful tool for predictive analysis and decision-making.

2.5 | FL Method

FL is a mathematical framework used for modeling situations where information is uncertain, imprecise, or involves linguistic variables instead of exact numerical values [45]. FL allows for a more human-like way of reasoning by accommodating degrees of truth rather than the traditional binary true/false paradigm [46]. Fuzzy modeling, based on the principles of FL, is particularly effective for addressing challenges where traditional models struggle, especially in predicting outcomes under uncertain conditions. A crucial aspect of FL systems is the use of membership functions, which define how each point in the input space is mapped to a membership value between 0 and 1. These values represent the degree to which an input belongs to a certain fuzzy set. Various types of membership functions can be employed, such as triangular, trapezoidal, and Gaussian functions, each suitable for different scenarios and capable of being integrated with a wide range of mathematical operators.

In this study, FL was utilized to model the relationships between five key input parameters: ID, LT, PS, NT, and RA. These inputs are critical factors in the 3D-printing process and significantly influence the mechanical properties of the printed material. The objective was to predict two important output variables: tensile strength and compressive strength of the printed specimens. The triangular membership function was selected to effectively capture the uncertainty and variability of the input parameters. This choice was made due to its simplicity and effectiveness in representing fuzzy intervals with minimal computational complexity. Applying the triangular membership function to the input parameters allowed for modeling gradual transitions between different input states, resulting in more accurate and reliable predictions of mechanical properties.

Figure 2 provides a detailed representation of the membership functions for both the input parameters and the output variables within the proposed FL framework. The fuzzy model is developed using a fuzzy inference system (FIS), which serves as the backbone for the implementation of FL principles. This system enables the mapping of input parameters to the desired outputs through a set of defined rules and membership functions. For the input parameters, a three-degree triangular membership function is employed. Each input—ID, LT, PS, NT, and RA—is associated with three linguistic variables: Low (L), Medium (M), and High (H). These linguistic terms allow the system to handle uncertainty and variability effectively by mapping numerical data into fuzzy sets. The triangular membership function is particularly chosen for its computational simplicity and ability to represent transitions between these linguistic categories with minimal overlap, ensuring smooth and interpretable fuzzy sets. For the output parameter, a seven-degree triangular membership function is proposed to provide finer granularity in describing the mechanical properties of the printed samples. The linguistic terms for the output are very low (VL), low (L), low medium (LM), medium (M), high medium (HM), high (H), and very high (VH). This higher degree of fuzzification enables a more precise classification of the results, which is crucial for evaluating the tensile and compressive strength of the specimens. The properties and specifications of the FIS are summarized in Table 5. These details provide a comprehensive overview of the fuzzy modeling approach and its ability to address the complexities of predicting mechanical properties in 3D-printed materials.

Figure 3 illustrates the triangular membership functions for all the parameters of this study, including both the inputs and the output utilized in the FIS of the proposed fuzzy modeling. In the FL modeling process, 120 If–Then rules were initially

TABLE 3 | L27 orthogonal array tensile and compressive test results.

Run	ID (%)	LT (μm)	PS (mm/s)	NT (°C)	RA (°)	Tensile strength (MPa)	Compressive strength (MPa)
1	30	100	40	190	0	21.13	31.01
2	30	100	40	190	45	18.24	28.54
3	30	100	40	190	90	16.35	26.31
4	30	200	60	200	0	17.87	26.93
5	30	200	60	200	45	15.42	24.85
6	30	200	60	200	90	13.83	22.92
7	30	300	90	210	0	15.46	23.31
8	30	300	90	210	45	13.36	20.15
9	30	300	90	210	90	11.71	18.27
10	60	100	60	210	0	21.87	32.88
11	60	100	60	210	45	18.89	30.08
12	60	100	60	210	90	16.97	27.65
13	60	200	90	190	0	17.62	26.81
14	60	200	90	190	45	15.23	24.64
15	60	200	90	190	90	13.63	22.70
16	60	300	40	200	0	21.77	32.78
17	60	300	40	200	45	18.81	30.04
18	60	300	40	200	90	16.91	27.65
19	90	100	90	200	0	20.05	30.09
20	90	100	90	200	45	17.33	27.12
21	90	100	90	200	90	15.50	24.48
22	90	200	40	210	0	24.32	36.73
23	90	200	40	210	45	20.99	32.62
24	90	200	40	210	90	18.42	28.97
25	90	300	60	190	0	19.67	29.91
26	90	300	60	190	45	17.05	26.88
27	90	300	60	190	90	15.24	24.23

TABLE 4 | The learning parameters used for ANN method.

Network type	Feed-forward backprop
Training function	Levenberg–Marquardt Training
Adaption learning function	Gradient Descent Learning
Performance function	Mean square error
Number of hidden layers	3
Number of neurons	30
Training method	Back-propagation
Number of epochs	900

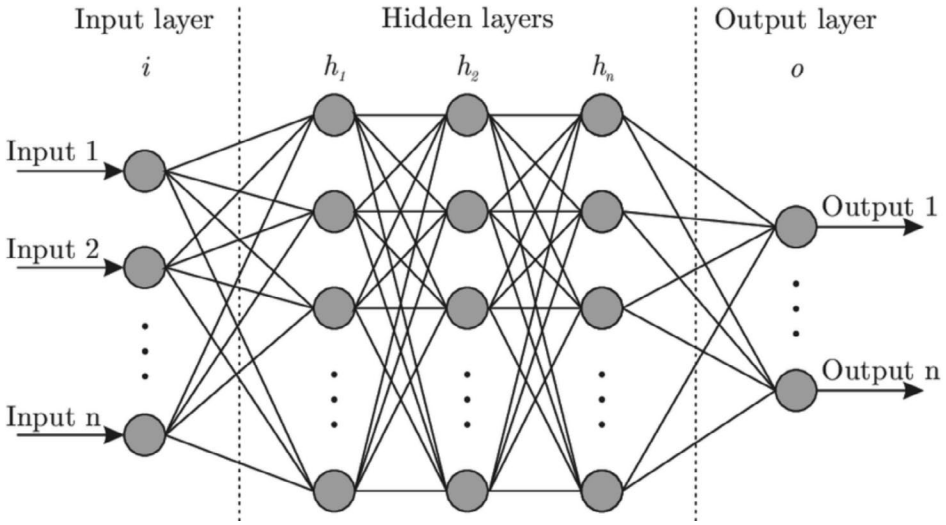

FIGURE 1 | Structure of the ANN model.

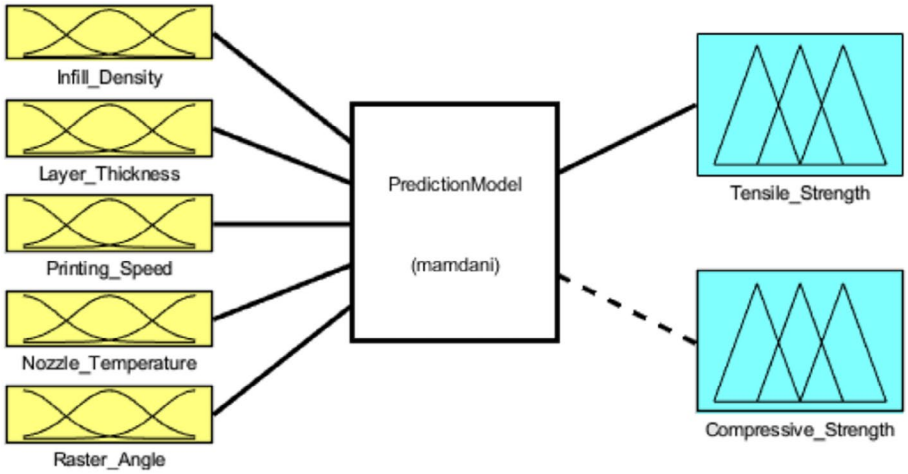

FIGURE 2 | Layout of the proposed fuzzy logic system with five inputs and two outputs.

considered, and the membership function values were calibrated based on the upper and lower limits of the inputs and outputs. These limits were refined using Taguchi, and rules for parameter relationships were established, leading to the formulation of rules defining the interactions among parameters. The fuzzy model was characterized by employing methods of minimum or maximum, with implications determined by the minimum, aggregation performed through the maximum, and defuzzification performed using the centroid method.

TABLE 5 | Properties of the proposed fuzzy logic FIS.

FIS type	Mamdani
Inputs–outputs	5–2
Membership functions	Triangular
Weight of rules	1
Number of rules	120
And method	Min
Implication method	Min
Aggregation method	Max
Defuzzification method	Centroid

3 | Results and Discussion

3.1 | Taguchi Design Results

In this section, the results of the Taguchi analysis are presented. Taguchi is widely adopted to enhance quality while reducing costs in product and process design. The average tensile and compressive strength values obtained from PLA/Wood composite samples fabricated using the FDM are presented in Table 3. The signal-to-noise (S/N) ratios were used to determine the optimal parameter settings, stabilize the process, and minimize variability. The experimental process employed the Taguchi L27 orthogonal array, consisting of 27 distinct experiments. For each sample, tensile and compressive strength was measured three times, and the average value is included in the table.

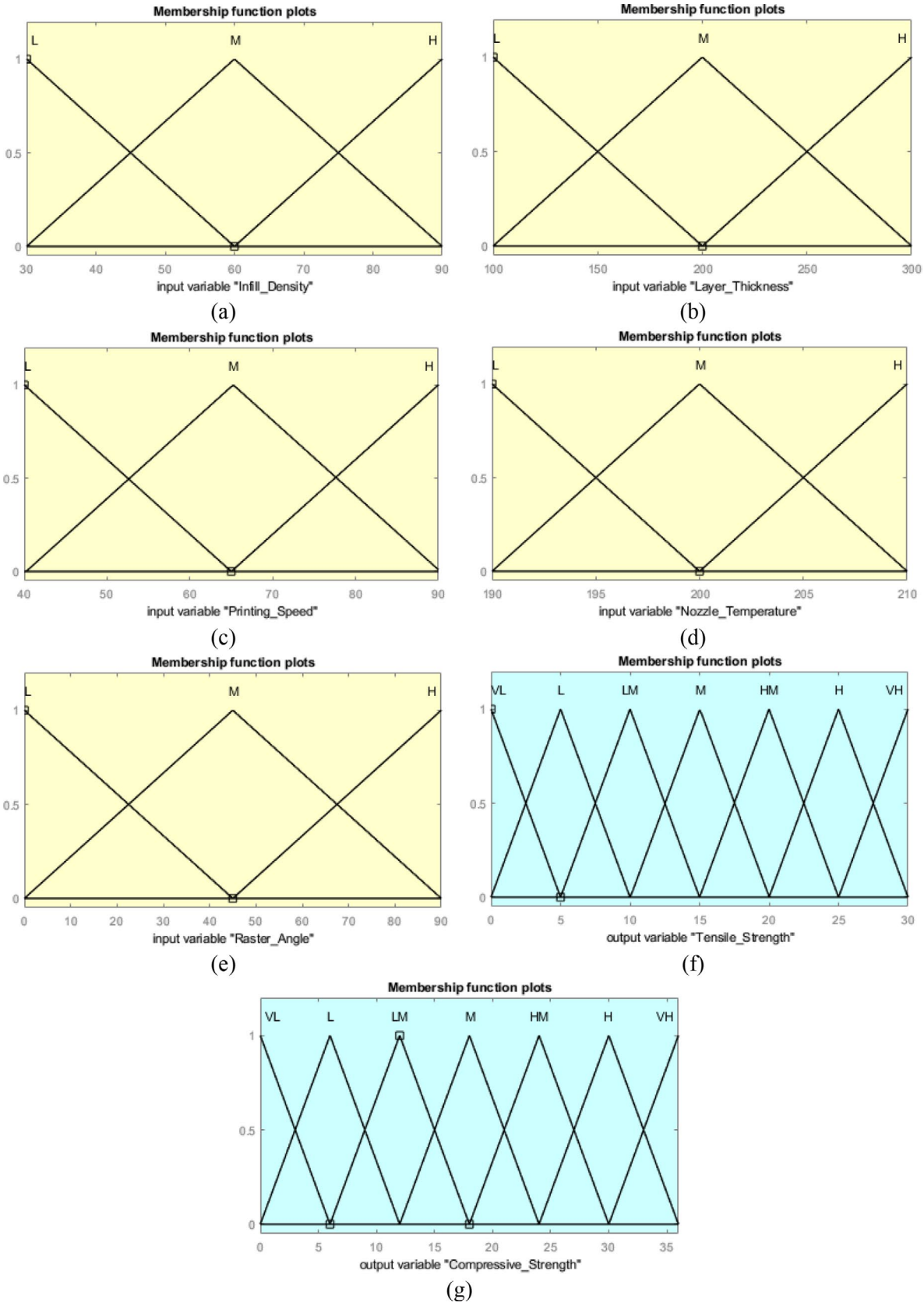

FIGURE 3 | Triangular membership functions of printing parameters and outputs.

The objective of this study was to predict the mechanical properties of composite samples fabricated under various printing conditions. The "larger is better" approach was applied to identify the parameter settings that yielded the highest strength values. In this study, the tensile and compressive strength values vary between 11.71–24.32–18.27 MPa and 18.27–36.73 MPa,

respectively, and the highest values were observed in Experiment 22. In this experiment, the printing parameters were set as follows: 90% ID, 200 μm LT, 40 mm/s PS, 210°C NT, and 0° RA. The recorded tensile and compressive strength values are 24.32 and 36.73 MPa, respectively. As expected, the experiment with the highest tensile and compressive strength also exhibited the highest S/N ratio. Higher S/N ratios indicate enhanced strength with minimal variability, signifying stable and optimal parameter configurations. Conversely, experiments yielding lower S/N ratios correspond to reduced strength or higher process variability, reflecting less optimal conditions. For instance, experiment 9, which exhibited one of the lowest tensile and compressive strengths (11.71 and 18.27 MPa), likely represents a less favorable combination of printing parameters. These findings underscore the importance of selecting appropriate settings to achieve consistent and desirable outcomes in FDM-based manufacturing processes.

The relationship between printing parameters and strengths was investigated using main effect graphs based on Taguchi's design (Figure 4). The effects on the tensile and compressive strength of the parameters were observed. The ID positively affects both types of strength. A significant increase in tensile and compressive strength was observed with the ID (30% → 90%). Especially at the ID of 90%, the highest SN ratios were obtained for both strengths. This shows that infill at high levels of data indicates that the samples are more durable. When the LT is evaluated, a decrease in the SN ratio was observed for the two types of strengths with the layer spacing (100 μm → 300 μm). This situation shows that the productions made with thinner layers show more positive results in both tensile and compressive strength. Especially at the LT of 100 μm, the optimum level of permanence was achieved for both types of strength. The PS has a negative structure on both strengths. PS characteristics (40 mm/s → 120 mm/s), tensile and compressive strengths decrease significantly. The lowest SN rates were observed at 120 mm/s. This shows that the strength of the samples increased at lower speeds. NT, the other effect comparison has a more limited protection feature. Both types of strengths showed a small increase from 190°C to 230°C, but this effect decreased to 240°C. Therefore, the effect of NT has a lower appearance compared to other effects. Finally, the RA caused a more significant decrease in compressive strength, leading to a similar decrease in tensile strength. Especially at the 90° RA, the lowest SN rates were obtained for both types of strength. In general, it was observed that lower RAs resulted in better strength results. As a result of these analyses, optimal results for both types of strength can be achieved with parameters such as 90% ID, 100 μm LT, 40 mm/s PS, 230°C NT, and 0° RA. In the experiments conducted using the optimum levels of the printing parameters, the tensile and compressive strength values were found to be 26.78 and 37.67 MPa, respectively.

In the 3D surface graphs, the effects of the printing parameters on tensile and compressive strength were clearly observed (Figure 5). ID had a positive effect on both types of strength, and the strength values increased significantly as the density increased. LT had a negative effect on both types of strength, and higher strength was obtained in samples produced with thinner layers. PS had a negative effect on strength, and higher strength values were observed at lower PSs. NT, although having a limited effect, increased the strength in a certain temperature range (190°C–230°C), but this effect decreased at higher temperatures. RA stood out as an important parameter, especially in compressive strength, and higher strength values were obtained at lower angles. The results observed in the surface graphs support and confirm the findings obtained in the main effects graphs. This analysis shows that the optimal parameter combinations (high ID, low LT, low PS, appropriate NT, and low RA) are effective in increasing both tensile and compressive strengths.

3.2 | Analysis of Variance

ANOVA was used to statistically understand the effects of printing parameters on tensile and compressive strength (Table 6). Since all factors have p value below 0.05, the effect of each parameter on strength is significant. While F value represents the magnitude of the effect of each factor, contribution percentages show the percentage distribution of these effects within the total variance. ID, the magnitude of the effect on tensile strength, was calculated as F value 176.93 and contribution rate 16.55%. It has a stronger effect on compressive strength with F value 153.49 and contribution rate 21.93%. This reveals that ID is a more significant factor especially in compressive strength. LT, F value 69.91 and contribution rate 6.54% for tensile strength, F value 54.93 and contribution rate 7.85% for compressive strength. Although the effect of LT is lower compared to other parameters, it has a statistically significant effect. PS is the most effective factor on both types of strength in terms of F value and additive ratios. F value is 358.68 and additive ratio is 33.55% for tensile strength, while F value is 286.38 and additive ratio is 40.92% for compressive strength. These results show that PS strongly affects both tensile and compressive strength. NT has a lower effect with F value of 16.12 and additive ratio of 1.51% for tensile strength and F value of 8.27 and additive ratio of 1.18% for compressive strength. This shows that NT has a more limited importance compared to other factors. RA was calculated as F value 447.55 and contribution rate 41.86% on tensile strength, and F value 196.82 and contribution rate 28.12% for compressive strength. This result reveals that RA is the most effective factor especially on tensile strength. R-squared values show the rate at which the model explains the variation in the dependent variables. The R-squared value for tensile strength is calculated as 99.26% and for compressive strength as 98.87%. These high R-squared values indicate that the model is quite robust, and the independent variables almost completely explain the variation in tensile and compressive strength.

3.3 | Results of ANN

When the difference between the expected and predicted outputs decreases below a specified tolerance level, or the number of training epochs exceeds a predetermined limit, the training process of the ANN is halted. This ensures the model does not overfit or continue training unnecessarily. A correlation coefficient (R value) close to 1 signifies a strong and consistent relationship between the predicted and actual data, reflecting the model's accuracy, while a value near 0 suggests a weak, inconsistent, or random correlation, indicating poor predictive

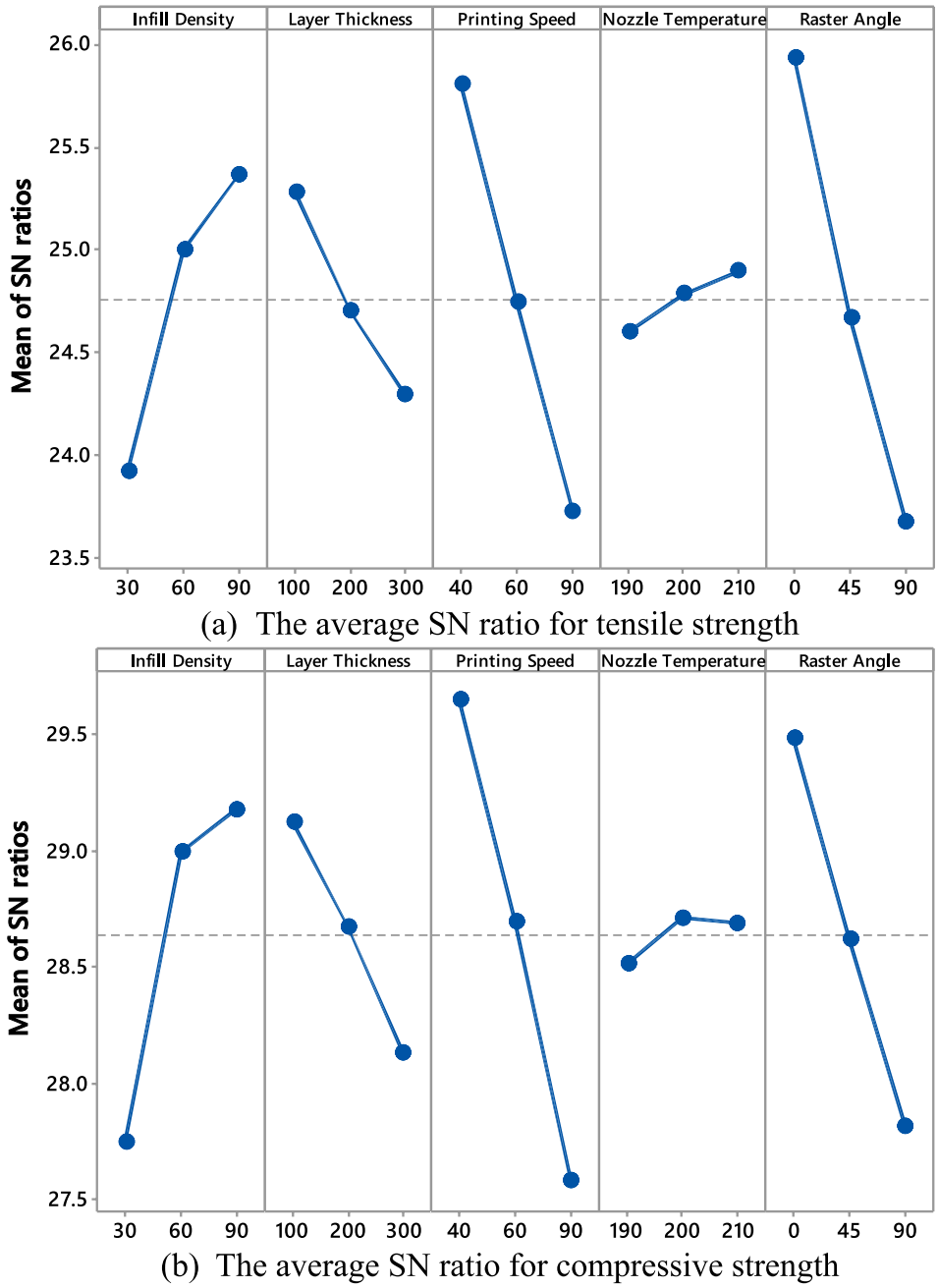

FIGURE 4 | Main effect plots of SN ratios for tensile and compressive strength.

performance. This approach balances computational efficiency with predictive accuracy, ensuring the ANN delivers reliable results aligned with the experimental data.

Figures 6 and 7 illustrate the regression graphs developed by ANN after 85 iterations for tensile strength and compressive strength, respectively. The regression plots obtained for tensile strength (Figure 6a) show correlation coefficients (*R* values) of 0.99824 for training, 0.99944 for validation, 0.98747 for testing, and 0.99536 for the total data. These values suggest an excellent fit, indicating that the ANN effectively captured the relationship between the input parameters and tensile strength. Similarly, the regression plots for compressive strength (Figure 6b) show *R* values of 0.98135 for training, 0.97165 for validation, 0.98241 for testing, and 0.97249 for the total data. These values are slightly lower than those for tensile strength but still demonstrate a strong correlation, confirming the ANN's ability to predict compressive strength accurately. The high correlation coefficients observed in both cases suggest that the ANN model's predicted outputs align closely with the experimental data, demonstrating its robustness and reliability for this application. Such strong performance indicates that the ANN model is well-suited to predict material properties based on the given input parameters. ANN performed satisfactorily with an average percentage error of 0.454% and 0.942% for tensile and compressive strength from the experimental results, indicating its potential for future use (Table 7). The maximum error amount was calculated as 1.95% in the experiments.

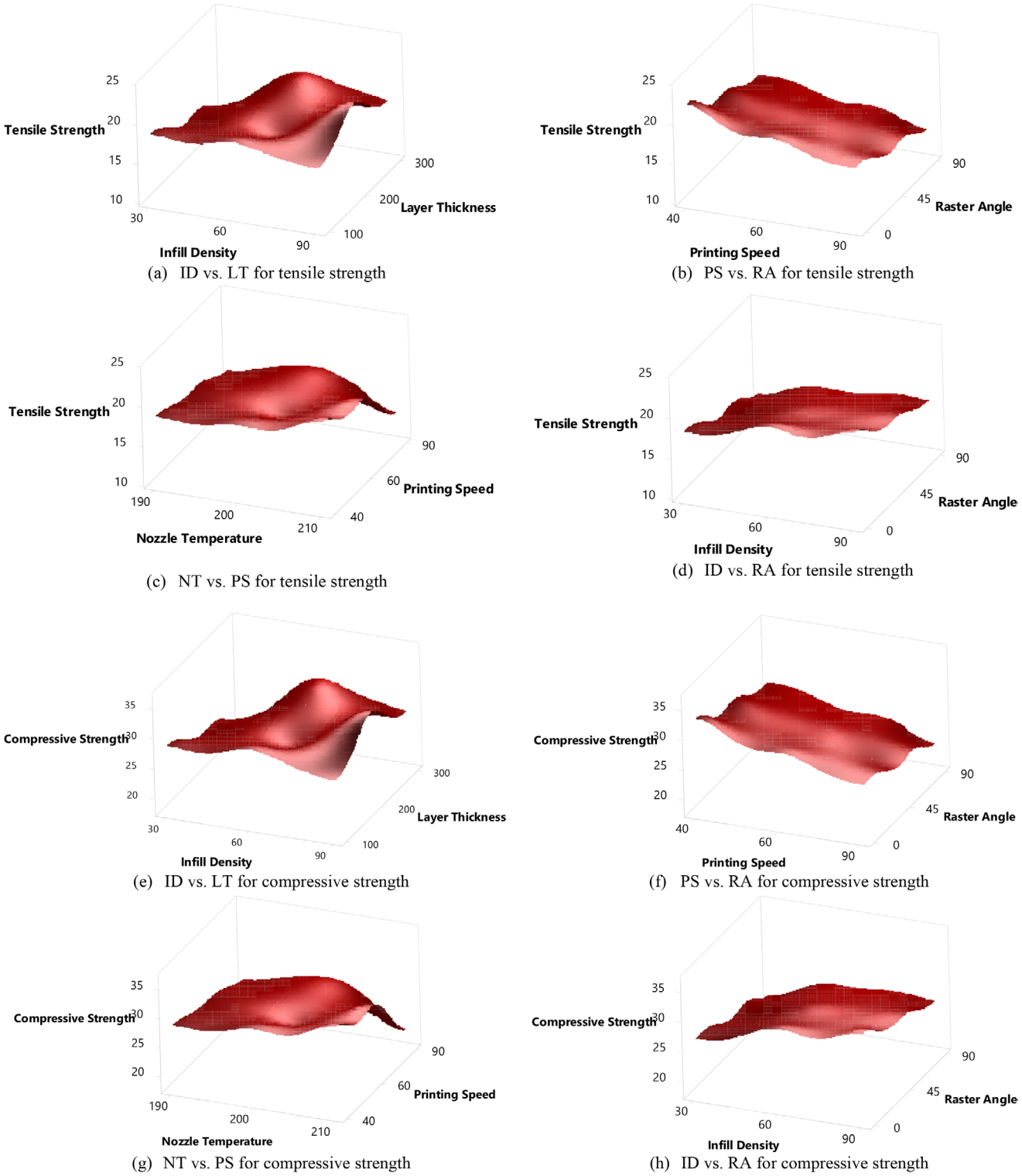

(a) ID vs. LT for tensile strength
(b) PS vs. RA for tensile strength
(c) NT vs. PS for tensile strength
(d) ID vs. RA for tensile strength
(e) ID vs. LT for compressive strength
(f) PS vs. RA for compressive strength
(g) NT vs. PS for compressive strength
(h) ID vs. RA for compressive strength

FIGURE 5 | 3D surface plots of tensile and compressive strength with factors.

3.4 | Results of FL

In this section, the results of the proposed FL model based on the Taguchi L27 orthogonal array experiment results have been obtained. This model was implemented using MATLAB R2019b software and 120 rules were created. After completing the FL modeling process, the defuzzification step was performed to determine a precise value for the output parameter. Subsequently, the predicted results from the model were compared with experimental data to assess their consistency and agreement.

The fuzzy modeling of the rules is given in Figure 7, where the experimental results, fuzzy predicted data from FIS, and the percentage error between each pair of data are demonstrated in Table 7. The results presented in the table indicate that the maximum errors for tensile and compressive strength predictions

TABLE 6 | ANOVA results for input–output parameters.

	Tensile strength				Compressive strength			
Factors	**Adj SS**	**Adj MS**	***F***	***p***	**Adj SS**	**Adj MS**	***F***	***p***
Infill density	37.712	18.856	176.93	0.000	97.017	48.5087	153.49	0.000
Layer thickness	14.902	7.4508	69.91	0.000	34.718	17.3591	54.93	0.000
Printing speed	76.452	38.226	358.68	0.000	181.011	90.5053	286.38	0.000
Nozzle temperature	3.431	1.7157	16.12	0.000	5.228	2.61427	8.27	0.003
Raster angle	95.394	47.697	447.55	0.000	124.402	62.2011	196.82	0.000
Degree of freedom	26				26			
R-squared	99.26%				98.87			

are 2.81% and 2.75%, respectively. These findings highlight the high accuracy and reliability of the fuzzy modeling system in capturing the complex relationships between input parameters and output responses. Such minimal error margins demonstrate that the FL approach is not only effective but also robust in situations where precise input data may be unavailable or difficult to obtain. Furthermore, this modeling strategy proves to be particularly advantageous when experimental analysis is challenging, time-consuming, or resource-intensive. FL enables researchers to derive dependable predictions and meaningful insights, making it a crucial resource for initial analyses, optimization efforts, and decision-making in a wide range of engineering and scientific disciplines.

3.5 | Comparative of Proposed Predictive Models

The results of 27 experiments performed as a result of Taguchi design were used to compare the prediction performance of two different methods. In the study, the tensile and compressive strength values, which are the two output parameters of the experiments, were predicted by ANN and FL methods. The comparison of actual and predicted tensile and compressive strength is shown in Figure 8. The ANN showed a lower error rate with a mean absolute error (MAE) value of 0.34 for tensile strength. On the other hand, the MAE value for the FL was calculated as 0.97. Similarly, the ANN showed better performance in compressive strength predictions, keeping the MAE value at 0.41, while this value was determined as 1.06 for the FL. The ANN drew a curve closer to the experimental data in both tensile and compressive strength predictions, while the FL showed higher deviations compared to the experimental data. These results reveal that the ANN is a more effective method in estimating both strength parameters.

In terms of standard error analysis, the results further support the superior performance of the ANN. For tensile strength predictions, the ANN demonstrated more consistent predictions with smaller deviations from the actual values, particularly at peak points (around experiment numbers 20–25). The standard error bands around the ANN predictions were notably tighter compared to those of the FL model, indicating higher prediction reliability. Similarly, for compressive strength estimations, the ANN maintained smaller standard error margins throughout the experimental range, especially evident in the regions of rapid strength variations (experiments 15–20). The FL exhibited wider standard error bands, showing greater uncertainty in its predictions, particularly at extreme values. This pattern of lower standard errors in the ANN model's predictions for both mechanical properties reinforces its statistical robustness and reliability as a prediction tool. The consistency in standard error performance across both tensile and compressive strength predictions suggests that the ANN provides more stable and dependable estimates of the material's mechanical properties.

Validation tests were conducted for the models developed based on ANN and FL to confirm their prediction accuracy. Five experimental studies were conducted outside the original design parameters but within the defined levels. Table 7 compares the success of ANN and FL in predicting both tensile and compressive strength depending on the specified input parameters. The table shows the error percentages between the actual values and the predicted values under different experimental conditions. The average error percentage of the ANN for tensile strength is quite low and the values generally vary between 0.53% and 1.25%. This shows that the ANN is very successful in predicting tensile strength. On the other hand, the error percentages for the FL are higher and vary between 0.95% and 2.81%. A similar result is observed for compressive strength. The ANN makes predictions with an average error of 0.94%, while the FL model has an average error rate of 2.00%. The low error percentages in the prediction performance of the ANN reveal that the model is better able to capture the relationship between the input and output parameters. In general, the average error rate of the ANN is around 0.74%, while this rate increases to 1.94% in the FL. These results clearly show that the ANN makes more precise and reliable predictions compared to the FL and exhibits superior performance, especially in data sets containing complex and nonlinear relationships.

3.6 | Discussion

The integration of natural fiber composites, particularly PLA/wood materials, in AM presents both opportunities and challenges in terms of understanding and optimizing their mechanical properties. This study's comprehensive approach to investigating and predicting the mechanical behavior of

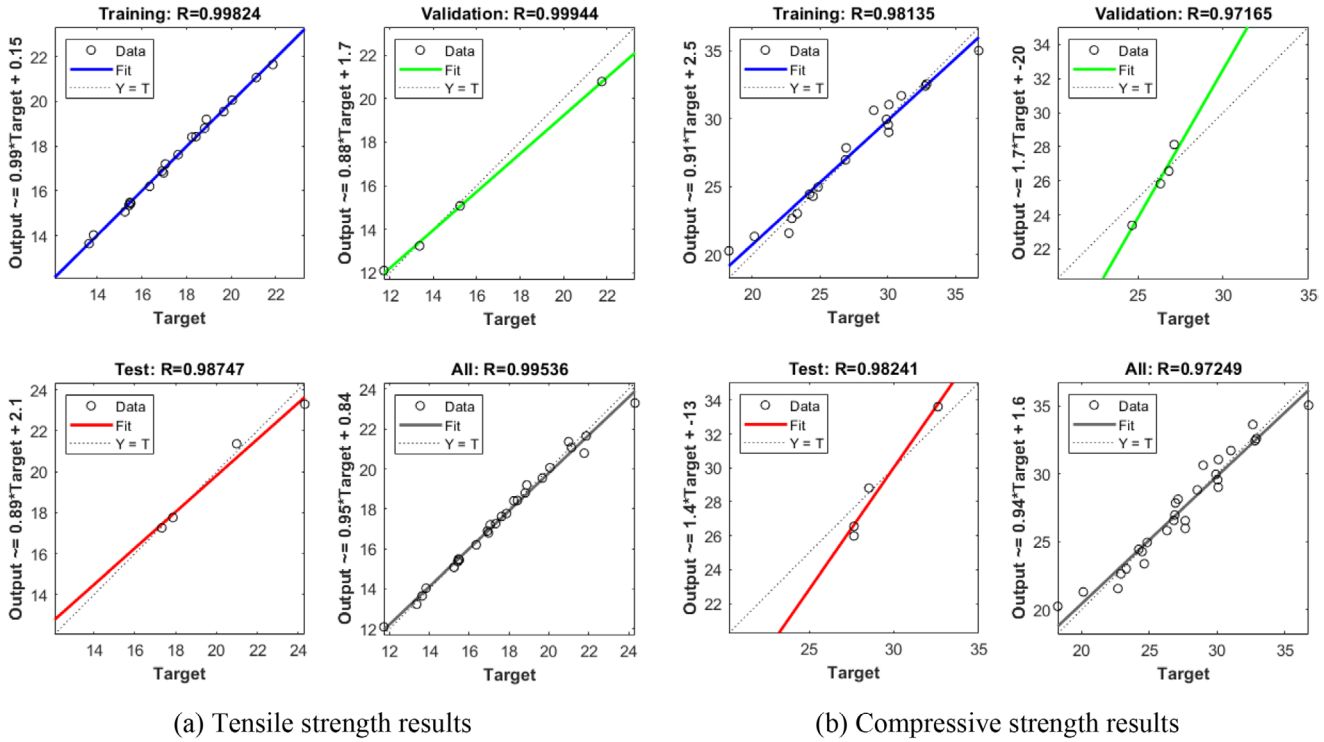

(a) Tensile strength results

(b) Compressive strength results

FIGURE 6 | Regression plots for tensile and compressive strength obtained using ANN.

FDM-printed PLA/wood composites provides valuable insights into both the manufacturing process and the effectiveness of predictive modeling techniques. The experimental results demonstrated that the mechanical properties of PLA/wood composites are significantly influenced by printing parameters, with RA and PS emerging as the most critical factors. The RA's dominant influence on tensile strength (41.86%) aligns with previous studies on fiber-reinforced composites, where fiber orientation plays a crucial role in load distribution and overall strength. This finding is particularly significant for wood-based composites, where the anisotropic nature of wood fibers adds complexity to the material's behavior. Similarly, the substantial impact of PS (40.92%) on compressive strength highlights the importance of proper material deposition and layer adhesion in achieving optimal mechanical properties.

The predictive modeling aspects of this study represent a significant advancement in the field of composite materials manufacturing. The exceptional performance of the ANN, achieving R^2 values of 99.94% for both tensile and compressive strength predictions, surpasses previously reported accuracy levels in similar studies. For instance, recent studies on FDM-printed composites typically reported prediction accuracies ranging from 85% to 95%. The notably low average error rate of 0.74% for the ANN model demonstrates the potential for precise property prediction without extensive experimental testing, which is particularly valuable for reducing development costs and time in industrial applications. The comparative analysis between ANN and FL models provides interesting insights into the capabilities of different predictive approaches. While both methods demonstrated high accuracy, the superior performance of ANN (MAE = 0.34 for tensile strength, 0.41 for compressive strength) compared to FL (MAE = 0.97 and 1.06, respectively) suggests that neural networks are particularly well-suited for capturing the complex, nonlinear relationships inherent in composite material behavior. This finding is especially relevant for wood-based composites, where material heterogeneity and processing parameters create intricate property–parameter relationships.

The validation results, showing maximum errors of 1.95% and 2.81% for ANN and FL respectively, demonstrate the robustness and reliability of these predictive models. These error rates are notably lower than those typically reported in the literature for similar materials and processes, where errors often range from 5% to 10%. This high level of accuracy is particularly significant for WPCs, where property prediction has traditionally been challenging due to the inherent variability of natural fibers and their interaction with polymer matrices. The optimization of printing parameters through the Taguchi method, combined with accurate predictive modeling, establishes a framework for efficient process parameter selection in FDM of PLA/wood composites. This integrated approach addresses a critical need in the field of sustainable manufacturing, where the ability to predict and optimize material properties without extensive trial-and-error experimentation is increasingly important. The findings particularly benefit industries focused on eco-friendly materials and sustainable manufacturing practices, where understanding and controlling the mechanical properties of natural fiber composites is crucial for their successful application.

Moreover, the study's findings have broader implications for the advancement of smart manufacturing and Industry 4.0 concepts. The successful implementation of AI-based prediction models demonstrates the potential for integrating intelligent systems into manufacturing processes, particularly for complex materials like WPCs. This integration can lead to more efficient production processes, reduced material waste, and improved product quality control. The comprehensive nature of this study,

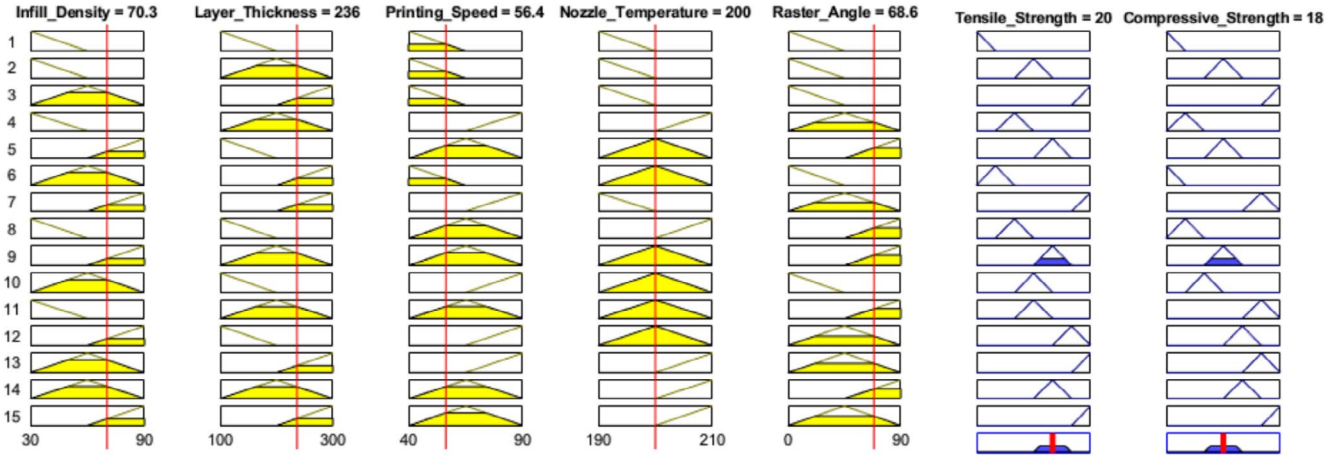

FIGURE 7 | Results of the rules for the given data in FL model.

TABLE 7 | Comparative evaluation of ANN and FL predictive models.

Output parameters	No	Input parameters ID (%)	LT (μm)	PS (mm/s)	NT (°C)	RA (°)	Actual	ANN Predicted	ANN %Error	FL Predicted	FL %Error
Tensile strength	1	0	300	60	210	45	13.36	13.28	0.53	13.14	1.58
	2	60	200	40	200	0	23.68	23.61	0.27	23.34	0.95
	3	90	100	40	190	90	20.03	19.77	1.25	19.59	2.17
	4	60	300	90	200	45	14.06	14.04	0.09	13.66	2.81
	5	90	200	60	210	0	20.93	20.91	0.13	20.52	1.93
Compressive strength	1	0	300	60	210	45	20.14	19.74	1.95	19.58	2.75
	2	60	200	40	200	0	35.81	35.47	0.93	29.62	1.69
	3	90	100	40	190	90	30.06	30.03	0.07	29.62	1.27
	4	60	300	90	200	45	21.96	21.66	1.34	21.43	2.39
	5	90	200	60	210	0	31.66	31.52	0.42	31.12	0.68

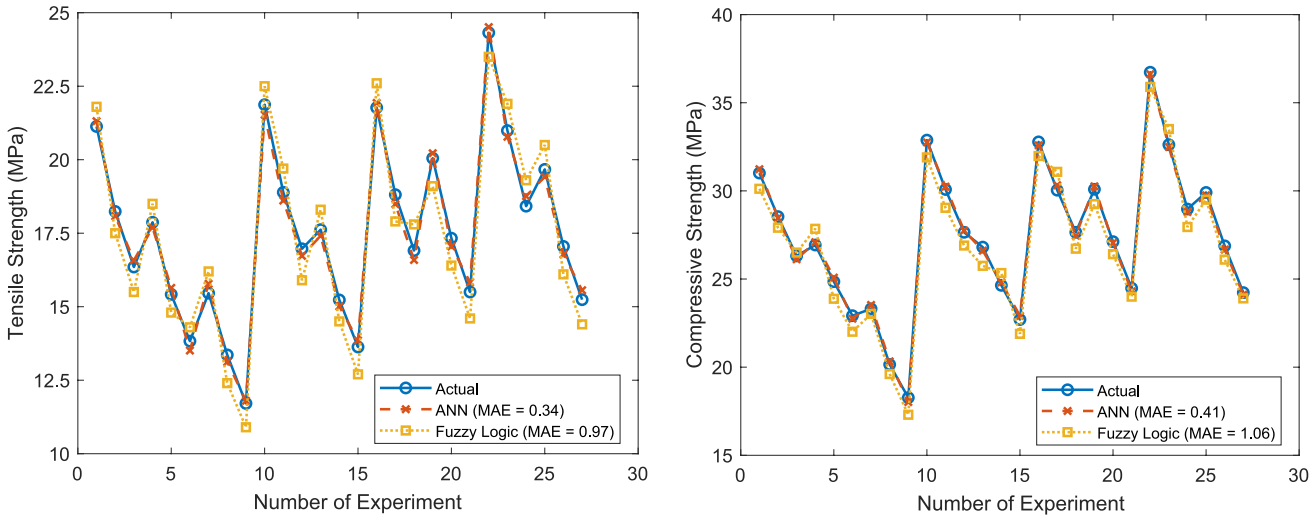

(a) Tensile strength results

(b) Compressive strength results

FIGURE 8 | Comparison of actual and predicted tensile and compressive strength.

combining experimental investigation with advanced predictive modeling, provides a valuable contribution to the field of composite materials manufacturing. The high prediction accuracies achieved demonstrate the potential for reducing reliance on extensive physical testing, while the detailed analysis of parameter effects offers practical guidance for optimizing manufacturing processes. These findings are particularly relevant as industries increasingly move toward sustainable materials and smart manufacturing practices, where efficient process optimization and reliable property prediction are essential for successful implementation.

4 | Conclusions

In this study, PLA/wood composite samples were fabricated using FDM, a widely utilized AM method renowned for its cost-efficiency, ease of implementation, and compatibility with various materials. The FDM process enabled precise control over critical parameters, facilitating a systematic investigation into their influence on the mechanical properties of the composite materials. The feasibility and efficacy of employing ANN and FL models to predict the mechanical properties of FDM-fabricated PLA/wood composites were demonstrated. The Taguchi experimental design was employed to thoroughly analyze the influence of five critical parameters—ID, LT, PS, NT, and RA—on tensile and compressive strengths. The RA emerged as the most influential factor for tensile strength, contributing 41.86%, while PS followed with a contribution of 33.55%. PS had the highest contribution at 40.92%, with RA contributing 28.12% for compressive strength. Statistical analyses using ANOVA confirmed the significance of all investigated factors (p value < 0.05), underscoring their critical roles in the FDM. These findings emphasize the necessity of optimizing RA and PS to achieve enhanced mechanical properties in PLA/wood composites. The predictive models developed through ANN and FL demonstrated high accuracy, with ANN exhibiting superior performance in both tensile and compressive strength predictions. The ANN model achieved an average error margin of 0.74%, compared to 1.94% for FL. For tensile strength predictions, ANN outperformed FL with a MAE of 0.34 versus 0.97. Similarly, for compressive strength, ANN achieved an MAE of 0.41, whereas FL had an MAE of 1.06. Notably, both models maintained error levels below 5%, a critical benchmark for ensuring the reliability and applicability of predictive models in engineering contexts. Keeping prediction errors within this threshold enables effective optimization of manufacturing parameters without extensive reliance on experimental iterations. Experimental validation further demonstrated the robustness of these models, with ANN achieving R^2 values exceeding 99% and FL models reaching up to 97%. This study underscores the potential of integrating advanced predictive modeling techniques with AM processes to optimize material properties and minimize experimental costs. This study highlights the potential of integrating advanced predictive modeling techniques with AM processes, particularly for optimizing the mechanical performance of PLA/wood composites produced via FDM, thereby advancing sustainable manufacturing practices and fostering the development of innovative, high-performance materials for industrial applications.

Ethics Statement

The authors have nothing to report.

Conflicts of Interest

The authors declare no conflicts of interest.

Data Availability Statement

All data underlying the results is available as part of the article and no additional source data is required.

References

1. M. Bhuvanesh Kumar and P. Sathiya, "Methods and Materials for Additive Manufacturing: A Critical Review on Advancements and Challenges," *Thin-Walled Structures* 159 (2021): 107228, https://doi.org/10.1016/j.tws.2020.107228.

2. M. Jayakrishna, M. Vijay, and B. Khan, "An Overview of Extensive Analysis of 3D Printing Applications in the Manufacturing Sector," *Journal of Engineering* 2023 (2023): 1–23, https://doi.org/10.1155/2023/7465737.

3. V. Bhatia, S. Sidharth, S. K. Khare, et al., "Intelligent Manufacturing in Aerospace: Integrating Industry 4.0 Technologies for Operational Excellence and Digital Transformation," Presented at the (2024).

4. S. C. Altıparmak and B. Xiao, "A Market Assessment of Additive Manufacturing Potential for the Aerospace Industry," *Journal of Manufacturing Processes* 68 (2021): 728–738, https://doi.org/10.1016/j.jmapro.2021.05.072.

5. H. R. Vanaei, S. Khelladi, and A. Tcharkhtchi, "3D Printing as a Multidisciplinary Field," in *Industrial Strategies and Solutions for 3D Printing* (Wiley, 2024), 1–24.

6. S. M. Desai, R. Y. Sonawane, and A. P. More, "Thermoplastic Polyurethane for Three-Dimensional Printing Applications: A Review," *Polymers for Advanced Technologies* 34 (2023): 2061–2082, https://doi.org/10.1002/pat.6041.

7. S. Nagaraja, P. B. Anand, K. Mohan Kumar, and M. I. Ammarullah, "Synergistic Advances in Natural Fibre Composites: A Comprehensive Review of the Eco-Friendly Bio-Composite Development, Its Characterization and Diverse Applications," *RSC Advances* 14 (2024): 17594–17611, https://doi.org/10.1039/D4RA00149D.

8. H. Ahmad, G. Chhipi-Shrestha, K. Hewage, and R. Sadiq, "A Comprehensive Review on Construction Applications and Life Cycle Sustainability of Natural Fiber Biocomposites," *Sustainability* 14, no. 23 (2022): 15905, https://doi.org/10.3390/su142315905.

9. D. Krapež Tomec and M. Kariž, "Use of Wood in Additive Manufacturing: Review and Future Prospects," *Polymers (Basel)* 14, no. 6 (2022): 1174, https://doi.org/10.3390/polym14061174.

10. M. Ramesh, L. Rajeshkumar, G. Sasikala, et al., "A Critical Review on Wood-Based Polymer Composites: Processing, Properties, and Prospects," *Polymers* 14, no. 3 (2022): 589, https://doi.org/10.3390/polym14030589.

11. T. S. Tamir, G. Xiong, Q. Fang, X. Dong, Z. Shen, and F.-Y. Wang, "A Feedback-Based Print Quality Improving Strategy for FDM 3D Printing: An Optimal Design Approach," *International Journal of Advanced Manufacturing Technology* 120 (2022): 2777–2791, https://doi.org/10.1007/s00170-021-08332-4.

12. J. Kechagias, D. Chaidas, N. Vidakis, K. Salonitis, and N. M. Vaxevanidis, "Key Parameters Controlling Surface Quality and Dimensional Accuracy: A Critical Review of FFF Process," *Materials and*

Manufacturing Processes 37 (2022): 963–984, https://doi.org/10.1080/10426914.2022.2032144.

13. O. Ulkir, "Investigation on the Mechanical and Thermal Properties of Metal-PLA Composites Fabricated by FDM," *Rapid Prototyping Journal* 30 (2024): 2113–2122, https://doi.org/10.1108/RPJ-01-2024-0007.

14. A. Kumar, A. R. Dixit, and S. Sreenivasa, "Mechanical Properties of Additively Manufactured Polymeric Composites Using Sheet Lamination Technique and Fused Deposition Modeling: A Review," *Polymers for Advanced Technologies* 35 (2024): e6396, https://doi.org/10.1002/pat.6396.

15. T. Manu, A. R. Nazmi, B. Shahri, N. Emerson, and T. Huber, "Biocomposites: A Review of Materials and Perception," *Materials Today Communications* 31 (2022): 103308, https://doi.org/10.1016/j.mtcomm.2022.103308.

16. F. Ferrari, R. Striani, D. Fico, M. M. Alam, A. Greco, and C. Esposito Corcione, "An Overview on Wood Waste Valorization as Biopolymers and Biocomposites: Definition, Classification, Production, Properties and Applications," *Polymers (Basel)* 14 (2022): 5519, https://doi.org/10.3390/polym14245519.

17. S. E. Van Nimwegen and P. Latteur, "A State-Of-The-Art Review of Carpentry Connections: From Traditional Designs to Emerging Trends in Wood-Wood Structural Joints," *Journal of Building Engineering* 78 (2023): 107089, https://doi.org/10.1016/j.jobe.2023.107089.

18. Y. Feng, H. Hao, H. Lu, C. L. Chow, and D. Lau, "Exploring the Development and Applications of Sustainable Natural Fiber Composites: A Review From a Nanoscale Perspective," *Composites. Part B, Engineering* 276 (2024): 111369, https://doi.org/10.1016/j.compositesb.2024.111369.

19. N. S. Balaji, C. Velmurugan, M. Saravana, M. Sivakumar, and P. Asokan, "Experimental Investigation on Mechanical Properties of FDM-Based Nylon Carbon Parts Using ANN Approach," *Surface Review and Letters* 30 (2023): 1–10, https://doi.org/10.1142/S0218625X23500282.

20. M. Ramesh, L. Rajeshkumar, and D. Balaji, "Influence of Process Parameters on the Properties of Additively Manufactured Fiber-Reinforced Polymer Composite Materials: A Review," *Journal of Materials Engineering and Performance* 30 (2021): 4792–4807, https://doi.org/10.1007/s11665-021-05832-y.

21. M. Stang, J. Tashman, D. Shiwarski, H. Yang, L. Yao, and A. Feinberg, "Embedded 3D Printing of Thermally-Cured Thermoset Elastomers and the Interdependence of Rheology and Machine Pathing," *Advanced Materials Technologies* 8 (2023): 2200984, https://doi.org/10.1002/admt.202200984.

22. J. F. Arinez, Q. Chang, R. X. Gao, C. Xu, and J. Zhang, "Artificial Intelligence in Advanced Manufacturing: Current Status and Future Outlook," *Journal of Manufacturing Science and Engineering* 142 (2020): 110804, https://doi.org/10.1115/1.4047855.

23. O. Ulkir and G. Akgun, "Prediction of Flexural Strength With Fuzzy Logic Approach for Fused Deposition Modeling of Polyethylene Terephthalate Glycol Components," *Journal of Materials Engineering and Performance* 33 (2024): 4367–4376, https://doi.org/10.1007/s11665-024-09291-z.

24. N. S. Johnson, P. S. Vulimiri, A. C. To, et al., "Invited Review: Machine Learning for Materials Developments in Metals Additive Manufacturing," *Additive Manufacturing* 36 (2020): 101641, https://doi.org/10.1016/j.addma.2020.101641.

25. Y. Wang, P. Zheng, T. Peng, H. Yang, and J. Zou, "Smart Additive Manufacturing: Current Artificial Intelligence-Enabled Methods and Future Perspectives," *Science China Technological Sciences* 63 (2020): 1600–1611, https://doi.org/10.1007/s11431-020-1581-2.

26. A. M. Babakan, M. Davoodi, M. Shafaie, M. Sarparast, and H. Zhang, "Predictive Modeling of Porosity in AlSi10Mg Alloy Fabricated by Laser Powder Bed Fusion: A Comparative Study With RSM, ANN, FL, and ANFIS," *International Journal of Advanced Manufacturing Technology* 129 (2023): 1097–1108, https://doi.org/10.1007/s00170-023-12333-w.

27. M. S. Meiabadi, M. Moradi, M. Karamimoghadam, et al., "Modeling the Producibility of 3D Printing in Polylactic Acid Using Artificial Neural Networks and Fused Filament Fabrication," *Polymers (Basel)* 13, no. 19 (2021): 3219, https://doi.org/10.3390/polym13193219.

28. G. Akgun and O. Ulkir, "Prediction Surface Roughness of 3D Printed Parts Using Genetic Algorithm Optimized Hybrid Learning Model," *Journal of Thermoplastic Composite Materials* 37 (2024): 2225–2245, https://doi.org/10.1177/08927057241243364.

29. J. A. Travieso-Rodriguez, R. Jerez-Mesa, J. Llumà, G. Gomez-Gras, and O. Casadesus, "Comparative Study of the Flexural Properties of ABS, PLA and a PLA–Wood Composite Manufactured Through Fused Filament Fabrication," *Rapid Prototyping Journal* 27 (2021): 81–92, https://doi.org/10.1108/RPJ-01-2020-0022.

30. D. Veeman and S. Palaniyappan, "Process Optimisation on the Compressive Strength Property for the 3D Printing of PLA/Almond Shell Composite," *Journal of Thermoplastic Composite Materials* 36 (2023): 2435–2458, https://doi.org/10.1177/08927057221092327.

31. E. Cuan-Urquizo, A. Álvarez-Trejo, A. Robles Gil, et al., "Effective Stiffness of Fused Deposition Modeling Infill Lattice Patterns Made of PLA-Wood Material," *Polymers (Basel)* 14, no. 2 (2022): 337, https://doi.org/10.3390/polym14020337.

32. D. Fico, D. Rizzo, V. De Carolis, F. Montagna, E. Palumbo, and C. E. Corcione, "Development and Characterization of Sustainable PLA/Olive Wood Waste Composites for Rehabilitation Applications Using Fused Filament Fabrication (FFF)," *Journal of Building Engineering* 56 (2022): 104673, https://doi.org/10.1016/j.jobe.2022.104673.

33. Y. Dong, J. Milentis, and A. Pramanik, "Additive Manufacturing of Mechanical Testing Samples Based on Virgin Poly (Lactic Acid) (PLA) and PLA/Wood Fibre Composites," *Advanced Manufacturing* 6 (2018): 71–82, https://doi.org/10.1007/s40436-018-0211-3.

34. N. A. Fountas, J. D. Kechagias, S. P. Zaoutsos, and N. M. Vaxevanidis, "Experimental and Statistical Study on the Effects of Fused Filament Fabrication Parameters on the Tensile Strength of Hybrid PLA/Wood Fabricated Parts," *Procedia Structural Integrity* 41 (2022): 638–645, https://doi.org/10.1016/j.prostr.2022.05.072.

35. O. Kelleci, D. Aydemir, E. Altuntas, et al., "Thermoplastic Composites of Polypropylene/Biopolymer Blends and Wood Flour: Parameter Optimization With Fuzzy-Grey Relational Analysis," *Polymers and Polymer Composites* 30 (2022): 1–10, https://doi.org/10.1177/09673911221100968.

36. A. Morvayová, N. Contuzzi, and G. Casalino, "Defects and Residual Stresses Finite Element Prediction of FDM 3D Printed Wood/PLA Biocomposite," *International Journal of Advanced Manufacturing Technology* 129 (2023): 2281–2293, https://doi.org/10.1007/s00170-023-12410-0.

37. E. Estakhrianhaghighi, A. Mirabolghasemi, L. Lessard, and A. Akbarzadeh, "3D Printed Wood-Fiber Reinforced Architected Cellular Composite Beams With Engineered Flexural Properties," *Additive Manufacturing* 78 (2023): 103800, https://doi.org/10.1016/j.addma.2023.103800.

38. M. D. Zandi, R. Jerez-Mesa, J. Lluma-Fuentes, J. J. Roa, and J. A. Travieso-Rodriguez, "Experimental Analysis of Manufacturing Parameters' Effect on the Flexural Properties of Wood-PLA Composite Parts Built Through FFF," *International Journal of Advanced Manufacturing Technology* 106 (2020): 3985–3998, https://doi.org/10.1007/s00170-019-04907-4.

39. W.-H. Chen, M. Carrera Uribe, E. E. Kwon, et al., "A Comprehensive Review of Thermoelectric Generation Optimization by Statistical Approach: Taguchi Method, Analysis of Variance (ANOVA), and Response Surface Methodology (RSM)," *Renewable and Sustainable Energy Reviews* 169 (2022): 112917, https://doi.org/10.1016/j.rser.2022.112917.

40. N. S. Patel, P. L. Parihar, and J. S. Makwana, "Parametric Optimization to Improve the Machining Process by Using Taguchi Method: A Review," *Materials Today Proceedings* 47 (2021): 2709–2714, https://doi.org/10.1016/j.matpr.2021.03.005.

41. H. T. Ünal and F. Başçiftçi, "Evolutionary Design of Neural Network Architectures: A Review of Three Decades of Research," *Artificial Intelligence Review* 55 (2022): 1723–1802, https://doi.org/10.1007/s10462-021-10049-5.

42. M. G. M. Abdolrasol, S. M. S. Hussain, T. S. Ustun, et al., "Artificial Neural Networks Based Optimization Techniques: A Review," *Electronics* 10, no. 21 (2021): 2689, https://doi.org/10.3390/electronics10212689.

43. A. Malekian and N. Chitsaz, "Concepts, Procedures, and Applications of Artificial Neural Network Models in Streamflow Forecasting," in *Advances in Streamflow Forecasting* (Elsevier, 2021), 115–147.

44. M. Adil, R. Ullah, S. Noor, and N. Gohar, "Effect of Number of Neurons and Layers in an Artificial Neural Network for Generalized Concrete Mix Design," *Neural Computing and Applications* 34 (2022): 8355–8363, https://doi.org/10.1007/s00521-020-05305-8.

45. M. Alateeq and W. Pedrycz, "Logic-Oriented Fuzzy Neural Networks: A Survey," *Expert Systems With Applications* 257 (2024): 125120, https://doi.org/10.1016/j.eswa.2024.125120.

46. J. Yadav, "Fuzzy Logic and Fuzzy Set Theory: Overview of Mathematical Preliminaries," in *Fuzzy Systems Modeling in Environmental and Health Risk Assessment* (Wiley, 2023), 11–29.